Contribution from the Department of Chemistry, Faculty of Science, Nagoya University, Chikusa-ku, Nagoya 464-01, Japan, Faculty of Pharmaceutical Sciences, Kanazawa University, Takara-machi, Kanazawa 920, Japan, and Coordination Chemistry Laboratories, Institute for Molecular Science, Myodaiji, Okazaki 444, Japan

Platinum DNA Intercalator–Mononucleotide Adduct Formation. Cooperativity between Aromatic Ring Stacking and Electrostatic Interactions

Akira Odani,[1a] Reiko Shimata,[1b] Hideki Masuda,[1c] and Osamu Yamauchi*,[1a]

Received September 4, 1990

Adduct formation by aromatic ring stacking and electrostatic interactions has been investigated for solutions containing platinum DNA intercalators $Pt(L)(en)^{2+}$ (L = 2,2′-bipyridine (bpy), 1,10-phenanthroline (phen), 5-nitro-1,10-phenanthroline (nphen), 3,4,7,8-tetramethyl-1,10-phenanthroline (Me_4phen); en = ethylenediamine) and mononucleotides NMP^{2-} (=AMP, GMP, CMP, UMP) or adenosine by spectroscopic methods. Difference absorption spectra of the $Pt(L)(en)^{2+}$–NMP^{2-} systems revealed spectral changes in the region 290–350 nm probably due to the stacking interaction between $Pt(L)(en)^{2+}$ and NMP^{2-}, which was supported by the induced circular dichroism (CD) peaks observed in this region. The stacking has been substantiated by ^{1}H NMR spectra, which exhibited upfield shifts ($\Delta\delta$) of the proton signals of the purine and pyrimidine rings and the H-1′ signal of the D-ribose moiety due to the ring current effect of coordinated L. The $\Delta\delta$ values were largest for $Pt(Me_4phen)(en)^{2+}$ (0.39–0.91 ppm for purine H-2 and H-8, 0.39–0.55 ppm for pyrimidine H-5 and H-6, and 0.49–0.71 ppm for ribose H-1′), implying that a large hydrophobic area is most effective for stacking. The stability constants log K were determined for the adducts $Pt(L)(en)^{2+}$–NMP^{2-}, where NMP^{2-} = AMP (L = bpy), GMP (L = bpy, Me_4phen), and CMP (L = bpy), and $Pt(bpy)(en)^{2+}$–adenosine from the absorption and CD spectra at pH 7–8 and 25 °C (I = variable, 0.1 M). The spectral data and the stability constants indicated cooperativity between the aromatic ring stacking and electrostatic interactions in adduct formation. Modes of interactions within the adducts in solution are discussed and compared with those in the solid state.

Weak intermolecular interactions are essential for molecular recognition in such specific biological bondings as nucleic acid–protein, enzyme–substrate, and neurotransmitter–receptor.[2] However, the very weakness of such interactions makes it difficult to specify their modes and energies. It has been shown by Lippard and his collaborators that platinum(II) complexes with large heteroaromatic rings (L) such as 2,2′-bipyridine and 1,10-phenanthroline intercalate into DNA base pairs.[3] Intercalation of planar compounds greatly influences the properties of DNA and is the first step in mutagenesis and drug actions.[4,5] Aromatic ring stacking between nucleobases and metal-coordinated L is considered to be the major driving force leading to intercalative binding of the above metallointercalators. The positive charge of the Pt(II) complexes may contribute to the binding through the electrostatic interaction with the negatively charged phosphate oxygens of DNA. Our preliminary circular dichroism (CD) and ^{1}H NMR spectral studies on the interactions of Pt(L)(en) (charges are omitted; en = ethylenediamine) with several mononucleotides (NMP) as fundamental constituents of nucleic acids indicated that the Pt(II) complexes have an intrinsic tendency to associate with nucleotides and nucleosides in dilute aqueous solution.[6,7] The extent of the association is expected to depend on the size and electron density of the interacting aromatic rings as well as the combined effect of hydrophobic and hydrophilic interactions in which solvents play an important role.[8] Ligand–ligand stacking interactions in ternary Cu(II)–amino acid[9–12] and Pd(II)–dipeptide complexes[13] involving aromatic nitrogen donors have been found to occur both in solution and in the solid state[14,15] and increase the stability of the resulting complexes in the order of the size of the rings involved in stacking.[11,13] On the other hand, electrostatic interactions between the oppositely charged side chains of coordinated amino acids have been concluded for a number of ternary Cu(II)[16,17] and Pd(II)[17c,d] complexes. Combination of hydrophobic and hydrophilic interactions may lead to cooperative effects on ligand–ligand or intermolecular interactions. With these points in mind we now studied intermolecular noncovalent interactions of several Pt(II) complexes Pt(L)(en) (L = bpy, phen, nphen, Me_4phen[18]) with various purine and pyrimidine bases of NMP (=AMP, GMP, CMP, UMP, Ado;[18] charges are omitted) in solution and in the solid state with a view to revealing the presence and mode of intermolecular associations between them.

Experimental Section

Materials. Ado, CMP, and UMP were obtained from Kohjin, AMP was obtained from Wako, and GMP was obtained from Sigma. D-Ribose 5-phosphate (barium salt) was purchased from Nacalai and used as the sodium salt solution made by adding Na_2SO_4 and removing $BaSO_4$ by filtration. Platinum(II) complexes $[Pt(en)_2]Cl_2$, $[Pt(bpy)(en)]Cl_2\cdot H_2O$, $[Pt(phen)(en)]Cl_2\cdot 2H_2O$, $[Pt(nphen)(en)]Cl_2\cdot 2H_2O$, and $[Pt(Me_4phen)(en)]Cl_2\cdot 3H_2O$ were prepared according to the literature[19] or

* To whom correspondence should be addressed.

(1) (a) Nagoya University. (b) Kanazawa University. (c) Institute for Molecular Science.
(2) (a) Frieden, E. *J. Chem. Educ.* **1975**, *52*, 754–761. (b) Jencks, W. P. *Adv. Enzymol. Relat. Areas Mol. Biol.* **1975**, *42*, 219–410. (c) Alberts, B.; Bray, D.; Lewis, J.; Raff, M.; Roberts, K.; Watson, J. D. *Molecular Biology of the Cell*, 2nd ed.; Garland Publishing: New York, 1989. (d) Watson, J. D.; Hopkins, N. H.; Roberts, J. W.; Steitz, J. A.; Weiner, A. M. *Molecular Biology of the Gene*, 4th ed.; Benjamin/Cummings: Menlo Park, CA, 1987.
(3) (a) Jennette, K. W.; Lippard, S. J.; Vassiliades, G. A.; Bauer, W. R. *Proc. Natl. Acad. Sci. U.S.A.* **1974**, *71*, 3839–3843. (b) Lippard, S. J.; Bond, P. J.; Wu, K. C.; Bauer, W. R. *Science* **1976**, *194*, 726–728. (c) Lippard, S. J. *Acc. Chem. Res.* **1978**, *11*, 211–217. (d) Barton, J. K.; Lippard, S. J. *Nucleic Acid-Metal Ion Interactions*; Spiro, T. G., Ed.; Wiley-Interscience: New York, 1980; pp 31–113.
(4) Waring, M. J. *Annu. Rev. Biochem.* **1981**, *50*, 159–192.
(5) Saenger, W. *Principles of Nucleic Acid Structure*; Springer-Verlag: New York, 1984.
(6) Yamauchi, O.; Odani, A.; Shimata, R.; Kosaka, Y. *Inorg. Chem.* **1986**, *25*, 3337–3339.
(7) Yamauchi, O.; Odani, A.; Shimata, R.; Ishiguro, S. *Recl. Trav. Chim. Pays-Bas* **1987**, *106*, 196–197.
(8) Baldini, G.; Varani, G. *Biopolymers* **1985**, *25*, 2187–2208.
(9) Fischer, B. E.; Sigel, H. *J. Am. Chem. Soc.* **1980**, *102*, 2998–3008.
(10) Yamauchi, O.; Odani, A. *Inorg. Chim. Acta* **1985**, *100*, 165–172.
(11) (a) Yamauchi, O.; Odani, A. *J. Am. Chem. Soc.* **1985**, *107*, 5938–5945. (b) Odani, A.; Yamauchi, O. *Nippon Kagaku Kaishi* **1987**, *336*–344.
(12) Sigel, H.; Tribolet, R.; Yamauchi, O. *Comments Inorg. Chem.* **1990**, *9*, 305–330.
(13) Odani, A.; Deguchi, S.; Yamauchi, O. *Inorg. Chem.* **1986**, *25*, 62–69.
(14) (a) Aoki, K.; Yamazaki, H. *J. Chem. Soc., Dalton Trans.* **1987**, 2017–2021. (b) Masuda, H.; Matsumoto, O.; Odani, A.; Yamauchi, O. *Nippon Kagaku Kaishi* **1988**, 783–788.
(15) Yamauchi, O.; Odani, A.; Kohzuma, T.; Masuda, H.; Toriumi, K.; Saito, K. *Inorg. Chem.* **1989**, *28*, 4066–4068.
(16) (a) Brookes, G.; Pettit, L. D. *J. Chem. Soc., Chem. Commun.* **1975**, 385–386. (b) Brookes, G.; Pettit, L. D. *J. Chem. Soc., Dalton Trans.* **1977**, 1918–1924.
(17) (a) Yamauchi, O.; Nakao, Y.; Nakahara, A. *Bull. Chem. Soc. Jpn.* **1975**, *48*, 2572–2578. (b) Sakurai, T.; Yamauchi, O.; Nakahara, A. *Bull. Chem. Soc. Jpn.* **1976**, *49*, 169–173, 1579–1584. (c) Yamauchi, O.; Odani, A. *J. Am. Chem. Soc.* **1981**, *103*, 391–398. (d) Yamauchi, O. *J. Mol. Catal.* **1984**, *23*, 255–261.
(18) The following abbreviations were used: bpy, 2,2′-bipyridine; phen, 1,10-phenanthroline; nphen, 5-nitro-1,10-phenanthroline; Me_4phen, 3,4,7,8-tetramethyl-1,10-phenanthroline; AMP, adenosine 5′-monophosphate; GMP, guanosine 5′-monophosphate; CMP, cytidine 5′-monophosphate; UMP, uridine 5′-monophosphate; Ado, adenosine.

0020-1669/91/1330-2133$02.50/0

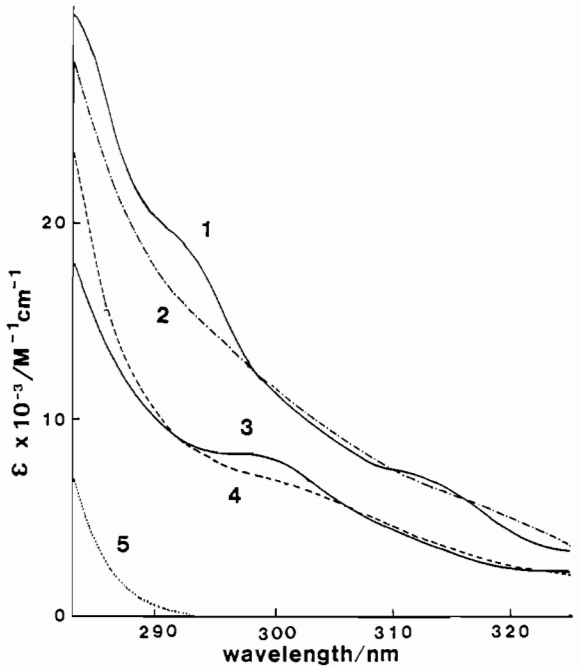

Figure 1. Absorption spectra of Pt(L)(en) in the presence and absence of AMP at pH 7–8. Curves: 1, Pt(Me_4phen)(en); 2, Pt(Me_4phen)(en)–AMP; 3, Pt(phen)(en); 4, Pt(phen)(en)–AMP; 5, AMP. Concentrations (mM): Pt(L)(en), 0.5; AMP, 5.0.

by similar methods. Preparation of [Pt(bpy)(en)]·AMP·10H_2O was reported earlier.[20]

Spectral Measurements. Absorption spectra were measured at room temperature in the range 220–400 nm with a Hitachi 330 recording spectrophotometer for aqueous solutions containing Pt(L)(en)Cl_2 (0.025 and 0.5 mM) (M = mol dm^{-3})) and NMP (0.03–0.7, 1.0, 5.0 mM) at pH 7–8. Difference spectra were obtained by subtracting from the spectrum of the ternary system the spectra of Pt(L)(en) and NMP measured under the same conditions. CD spectra were measured in the same range with a JASCO J-500C spectropolarimeter for aqueous solutions contg. Pt(L)(en)Cl_2 (0.5 mM) and NMP (0.5–5.0 mM). The CD spectra were also recorded at various ionic strengths I (= variable, 0.1, 0.5, 1.0 M ($NaClO_4$)). ^{1}H NMR spectra were measured for solutions of 1:1 Pt(L)(en)Cl_2–NMP (20 mM for L = bpy and 10 mM for L = all others) in D_2O (99.8%) with 3-(trimethylsilyl)propionate (TSP), *tert*-butyl alcohol, or dioxane as internal standard. In other measurements the concentrations of both Pt(L)(en)Cl_2 and NMP were varied in the range 10–200 and 7.5–200 mM, respectively. The spectra were obtained at 25, 35, 50, and 75 °C with a JEOL FX-100 NMR spectrometer in the FT mode.

X-ray Crystal Structure Determination. Procedures for the X-ray structural determination have been reported in a previous paper.[20] Tables of atomic coordinates, anisotropic thermal parameters, bond distances and angles, torsion angles, and observed and calculated structure factors are available from the authors upon request.

Results

Absorption and CD Spectra. The Pt(II) complexes Pt(L)(en) have absorption peaks in the region 290–340 nm at pH 7–8. Addition of NMP caused spectral changes in this region, indicating the interactions between Pt(L)(en) and NMP (Figure 1). The difference spectra revealed that the spectral changes occurred in the absorption band of L and the charge-transfer (CT) region as shown for Pt(bpy)(en)–AMP in Figure 2. Interestingly no changes were observed for Pt$(en)_2$–NMP and Pt(L)(en)–D-ribose 5-phosphate systems, which have no possibility of stacking interactions. The Pt(L)(en)–AMP systems gave positive CD peaks in the region 280–350 nm, where NMP's did not show appreciable CD bands but where the systems showed absorption spectral changes. This is most probably because of the proximity effect of the optically active D-ribose moiety located close to the Pt(II) center and is in accordance with the results obtained for Pt(bpy)(en)–NMP (NMP = AMP, GMP) and Pt(bpy)(en)–Ado reported earlier.[6] The CD spectral magnitudes depend on the ratio of NMP to Pt(L)(en), indicating the equilibrium of the Pt(L)(en)–NMP adduct formation (Table I). No CD band was observed for the systems lacking absorption spectral changes. The CD spectra for the Pt(bpy)(en)–GMP system with added $NaClO_4$ (0–0.5 M) as well as the previous results[6] for Pt(bpy)(en)–AMP showed that the CD peaks are affected by the ionic strength (I) of the medium.

Table I. CD Spectral Data for Pt(L)(en)–AMP Systems in Water at ≥280 nm

Pt(L)(en)[a]	concn of AMP/mM	pH	λ_{max}/nm ($\Delta\epsilon$/(M of Pt)$^{-1}$ cm^{-1})
Pt(Me_4phen)(en)	0.5	7.3	293 (+1.47)
	2.5	7.6	294 (+1.58)
	5.0	7.7	294 (+2.60)
Pt(phen)(en)	0.5	7.2	285 (+0.36)
	2.5	7.6	287 (+1.16)
	5.0	7.7	290 (+1.18)
Pt(bpy)(en)	0.5	7.7	320 (+0.45)
	2.5	7.8	320 (+0.84)
	5.0	7.8	320 (+1.15)
Pt(nphen)(en)	0.5	7.2	315 (+0.30)
	2.5	7.4	305 (+0.61)
	5.0	7.5	300 (+0.76)

[a] Concentration of Pt(II) Complexes: 0.5 mM.

^{1}H NMR Spectra. When NMP interacts with Pt(L)(en) through stacking, upfield shifts ($\Delta\delta$) of the signals of the nucleobase are expected to be caused by the ring current effect[21] of L, which may serve as a good indication of stacking. In a previous NMR study[13] we detected upfield shifts due to intramolecular aromatic ring stacking in the ternary Pd(II) complexes containing phen, bpy, etc. and a dipeptide with an aromatic side chain. ^{1}H NMR spectra have been extensively studied by Sigel et al. for substantiating the intramolecular hydrophobic or stacking interactions in ternary metal complexes between coordinated phen or bpy and an aromatic or aliphatic side group of the other ligand.[9,22]

The NMR spectral data for Pt(L)(en), NMP, and Ado systems and the systems involving both the Pt(II) complexes and NMP or Ado in D_2O at pD 7–8 are summarized in Table II. While there were no shifts of the signals upon mixing Pt$(en)_2$ with NMP, upfield shifts were detected for the 1:1 Pt(L)(en)–NMP or –Ado systems (20 mM). Since the signals for Pt(L)(en)–NMP (or Ado) systems correspond well with those of Pt(L)(en) and NMP (or Ado) except for the shifts, it is evident that Pt(L)(en) retains its coordination structure before and after mixing with NMP or Ado. In the presence of Pt(Me_4phen)(en) the H-2 and H-8 signals of the purine bases at 8–8.5 ppm and the H-1′ signal of D-ribose at ~6.2 ppm exhibited upfield shifts of 0.39–0.91 ppm. The H-5 (~6.2 ppm), H-6 (~8.1 ppm), and H-1′ (~6.0 ppm) signals of pyrimidine nucleotides also shifted upfield by 0.36–0.71 ppm. Large shifts were observed for Pt(Me_4phen)(en) having the largest hydrophobic area, whereas the shifts for L = bpy were the smallest. Pt(nphen)(en) caused shifts of the purine base signals that were larger than those observed for Pt(bpy)(en) and Pt(phen)(en), which may suggest that the electron-withdrawing effect of the

(19) (a) Basolo, F.; Bailar, J. C., Jr.; Tarr, B. R. *J. Am. Chem. Soc.* **1950**, *72*, 2433–2438. (b) Morgan, G. T.; Burstall, F. H. *J. Chem. Soc.* **1934**, 965–971. (c) Palocsay, F. A.; Rund, J. V. *Inorg. Chem.* **1969**, *8*, 524–528. (d) McFadyen, W. D.; Wakelin, L. P. G.; Roos, I. A. G.; Leopold, V. A. *J. Med. Chem.* **1985**, *28*, 1113–1116.
(20) Masuda, H.; Yamauchi, O. *Inorg. Chim. Acta* **1987**, *136*, L29.
(21) (a) Johnson, C. E., Jr.; Bovey, F. A. *J. Chem. Phys.* **1958**, *29*, 1012–1014. (b) Bovey, F. A. *Nuclear Magnetic Resonance Spectroscopy*; Academic: New York, 1969.
(22) (a) Chaudhuri, P.; Sigel, H. *J. Am. Chem. Soc.* **1977**, *99*, 3142–3150. (b) Mitchell, P. R.; Sigel, H. *J. Am. Chem. Soc.* **1978**, *100*, 1564–1570. (c) Fukuda, Y.; Mitchell, P. R.; Sigel, H. *Helv. Chim. Acta* **1978**, *61*, 638–647. (d) Scheller, K. H.; Hofstetter, F.; Mitchell, P. R.; Prijs, B.; Sigel, H. *J. Am. Chem. Soc.* **1981**, *103*, 247–260. (e) Sigel, H.; Scheller, K. H.; Scheller-Krattiger, V.; Prijs, B. *J. Am. Chem. Soc.* **1986**, *108*, 4171–4178. (f) Sigel, H. *Pure Appl. Chem.* **1989**, *61*, 923–932.

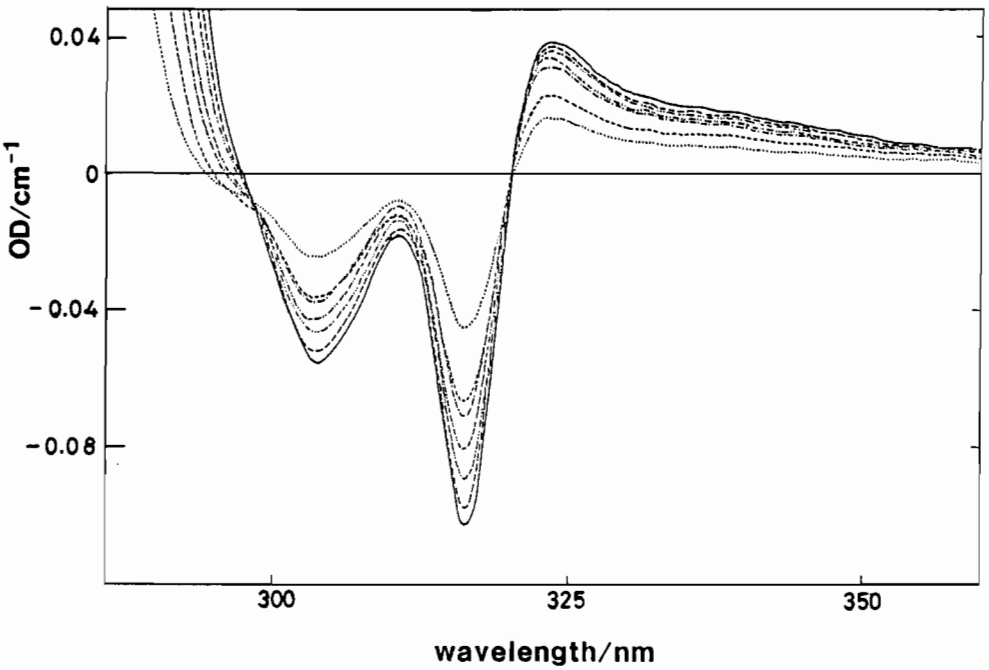

Figure 2. Difference spectra for Pt(bpy)(en)–AMP systems at pH 7.5–7.7. Concentrations (mM): Pt(bpy)(en), 0.025; AMP, 0.65 (···), 1.30 (- - -), 1.95 (-·-), 2.68 (-··-), 3.57 (-···-), 4.47 (– – –), 5.36 (—).

Table II. ^{1}H NMR Chemical Shifts (δ),[a] Coupling Constants (J),[b] and Upfield Shifts ($\Delta\delta$) for 20 mM 1:1 Pt(L)(en)–NMP Systems at pD 6–8

				Pt(L)(en)								
		no Pt(L)(en)		bpy		phen		Me_4phen		nphen	en	
NMP	H	δ	J	$\Delta\delta$	J	$\Delta\delta$	J	$\Delta\delta$	J	$\Delta\delta$	$\Delta\delta$	J
AMP	8	8.61		0.15				0.45		0.45	0.00	
	2	8.24		0.29				0.91		0.57	0.00	
	1′	6.14	6.1	0.17	5.9			0.71	4.2	0.39	0.00	6.1
AMP[c]	8	8.58				0.22						
	2	8.29				0.38						
	1′	6.13	6.1			0.27	4.9					
GMP	8	8.21		0.14[d]		0.13		0.39		0.34		
	1′	5.93	6.4	0.16[d]		0.38	3.9	0.55		0.40		
CMP	6	8.13	7.5	0.16	7.6	0.29	7.4	0.55	7.6			
	5	6.15	7.5	0.18	7.6	0.34	7.4	0.43	7.6			
	1′	6.02	3.4	0.10	3.7[e]	0.21	4.0[e]	0.71	4.0[e]			
UMP	6	8.13	8.0	0.05		0.22		0.39	8.1			
	5	5.99	8.0	0.02		0.23		0.36	8.1			
	1′	6.01	4.6	0.04		0.21		0.49	3.7			
Ado	8	8.31		0.03		0.12						
	2	8.20		0.11		0.11						
	1′	6.06	6.1	0.04		0.13	6.1					

[a] Downfield in ppm relative to TSP. [b] Hz. [c] Measured at 70 °C. [d] Measured at 50 °C. [e] Uncertainties due to signal overlapping.

NO_2 group makes the stacking interaction between Pt(nphen)(en) and NMP more effective.[11b] The methyl signals for Pt(Me_4phen)(en) were much less shifted upfield in the presence of AMP and GMP, $\Delta\delta$ values being 0.03–0.10 ppm. This indicates that the stacked nucleobases do not overlap with the methyl groups situated outside the phen ring.

The upfield shifts observed for the H-2, H-8, and H-1′ signals in the 1:1 Pt(L)(en)–AMP systems (L = bpy, Me_4phen) decreased with the increase of the ionic strength (I) adjusted with KNO_3 (Table III), which implies that electrostatic interactions also contribute to the Pt(L)(en)–NMP adduct formation.

Temperature and Concentration Dependence of the ^{1}H NMR Spectra. The noncovalent interactions between Pt(L)(en) and NMP are expected to be weakened at high temperatures, because the large negative enthalpy change revealed by a previous calorimetric study[7] indicates that the adduct is more stable at lower temperatures. The temperature dependence of the spectrum of the 1:1 Pt(bpy)(en)–AMP system was measured at 25–75 °C. The H-2, H-8, and H-1′ signals of AMP and the β-H signals of bpy exhibited smaller $\Delta\delta$ values at higher temperatures, indicating that the stacking is less effective at elevated temperatures. In

Table III. Ionic Strength (I) Dependences of Upfield Shifts ($\Delta\delta$) Observed for AMP in 1:1 Pt(L)(en)–AMP Systems at 25 °C

	$\Delta\delta$/ppm				
	L = bpy (20 mM) I (KNO_3)			L = Me_4phen (10 mM) I (KCl)	
AMP H	var[a]	0.1	1.0	var[a]	0.1
H-2	0.29	0.21	0.17	0.91	0.77
H-8	0.15	0.12	0.08	0.45	0.37
H-1′	0.17	0.13	0.10	0.71	0.65

[a] Var = variable.

accordance with the concentration dependence of the CD spectral magnitude (Table I), the $\Delta\delta$ values for the Pt(bpy)(en)–AMP and –CMP systems increased with the increase of concentration (Figure 3). In measuring the concentration dependence, we avoided the effect of self-stacking of NMP by selecting the concentrations of 7.5 mM for AMP and 20 mM for CMP, where the self-stacked dimers are estimated to be less than 5% from the equilibrium constants reported in the literature.[22d,23] The observed

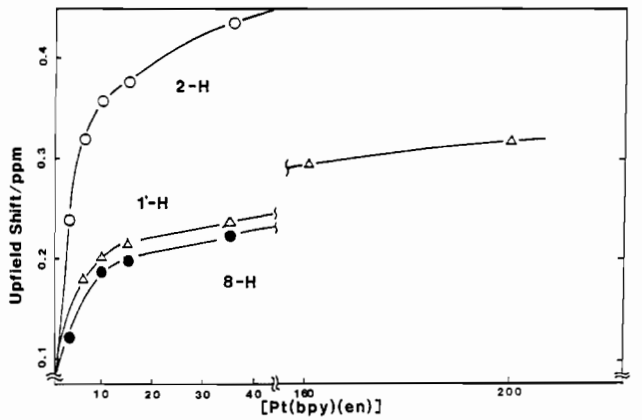

Figure 3. Concentration dependence of upfield shifts of AMP proton signals for Pt(bpy)(en)–AMP systems in D_2O. Concentration of AMP: 7.5 mM.

Table IV. Apparent Stability Constants, log K, of Pt(L)(en)–NMP Complexes at 25 °C and pH 6–8

NMP	L	log K^a	I/M^b	method^c	remarks
AMP	bpy	2.3 (4)	0.1	UV	this work
	bpy	2.30 (7)	0.1	cal	*d*
	bpy	2.82 (7)	var	UV	*d*
	phen	2.51 (3)	0.1	cal	*d*
	phen	3.18 (8)	var	UV	*d*
	Me_4phen	3.07 (8)	0.1	cal	*d*
	Me_4phen	3.47 (8)	var	CD	*d*
GMP	bpy	2.59 (3)	var	UV	this work
	Me_4phen	3.5 (1)	var	CD	this work
CMP	bpy	2.5 (2)	var	UV	this work
Ado	bpy	1.9 (2)	0.1	UV	this work

[a] Values in parentheses denote standard deviations. [b] Ionic strength (I) was adjusted with $NaClO_4$ (for UV) and NaCl (for cal). [c] log K values were calculated from the absorption (UV) or CD (CD) spectra or calorimetry (cal). [d] Reference 7.

$\Delta\delta$ increase is therefore mainly due to the increase of the adduct concentration. Figure 3 clearly shows that higher concentrations are more favorable for intermolecular interactions. The steep rise of the curves at the Pt(II) complex concentrations of ~15 mM indicates that the adduct is formed to a greater extent at the [Pt(bpy)(en)]/[AMP] ratio of ~2. The order of the $\Delta\delta$ values, H-2 > H-1′ > H-8 for AMP and H-5 > H-6 > H-1′ for CMP, are unaffected by the concentration ratios, showing that the relative position of the stacked rings remains the same at different concentrations.

Equilibrium of Adduct Formation. Since Pt(L)(en) and NMP interact with each other only through noncovalent bonds, the stability of the adduct is expressed by the following equilibrium:

$$\text{Pt(L)(en)} + \text{NMP} \overset{K}{\rightleftharpoons} \text{Pt(L)(en)–NMP}$$

The stability constants log K were calculated from the absorption and CD spectra at 25 °C and pH 6–8 (I = variable, 0.1 M ($NaClO_4$)) by nonlinear least-squares curve fitting for the systems with AMP[7] and GMP showing spectral changes due to the interaction. The log K values for Pt(bpy)(en)–AMP and –GMP were also obtained by Benesi–Hildebrand plots. Induced CD spectral magnitudes were used for Pt(Me_4phen)(en)–NMP. Reliable stability constants were not obtained by spectral methods for the systems with CMP and UMP, which did not show large spectral changes necessary for the calculation. The log K values determined in the present and previous[6,7] studies are listed in Table IV, where we see that the adduct stabilities correspond well with the CD spectral magnitudes and the $\Delta\delta$ values of the NMR spectra.

(23) Tribolet, R.; Sigel, H. *Biophys. Chem.* **1987**, *27*, 119–130.

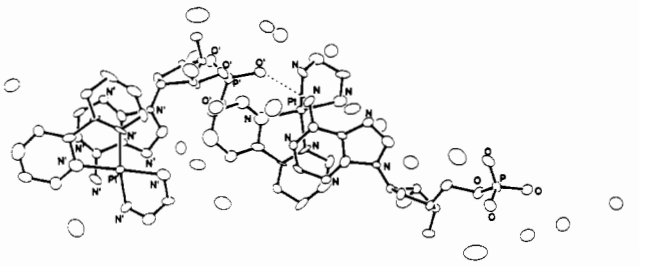

Figure 4. Crystal structure of [Pt(bpy)(en)]·AMP·10H_2O, showing the stacking and hydrogen bonding. The primed and unprimed atoms are related by the crystallographic screw axis.

Discussion

Intermolecular Interactions in Solution. The CT band due to stacking in the ternary systems Cu(phen)(NMP) has been reported to appear in the region 300–400 nm.[24] The spectral changes observed for the Pt(L)(en)–NMP systems in the ultraviolet region are most probably due to the CT arising from similar stacking between coordinated L and the base moiety of NMP. Pt(bpy)$(NH_3)_2$ sandwiched between the two benzene rings of dibenzo-30-crown-10[25] has been reported to give a CT band at ~350 nm.[25] The $\Delta\delta$ values for the purine nucleotides in Table II show that the magnitudes of the upfield shifts, which are greater for greater interacting aromatic rings, are in the order H-2 > H-1′ > H-8 irrespective of the structure of L with the exception of nphen. Interestingly, Ado which is devoid of the negatively charged phosphate group exhibited much smaller $\Delta\delta$ values than those of AMP. Since the Pt(L)(en)–D-ribose 5-phosphate systems failed to exhibit the induced CD bands, stacking seems to be the driving force for the Pt(II) complex–NMP association, and the electrostatic interaction between Pt^{2+} and $-OPO_3^{2-}$ and possibly the hydrogen bonding between coordinated NH_2 and $-OPO_3^{2-}$ may contribute to adduct formation and positioning NMP relative to the Pt(L)(en) molecule only when NMP is bound by stacking. The ionic strength dependence of the CD magnitude showed that there exists such interactions, and the upfield shifts of the ^{31}P NMR signal of AMP due to Pt(bpy)(en) also point to the proximity of the phosphate group to Pt(II).[6] This is further supported by the X-ray analysis of copper(II) complexes showing that the GMP and the IMP (= inosine 5′-phosphate) phosphate group is hydrogen bonded to the water molecule apically coordinated to Cu(II).[26] The hydrogen bonding that has been detected between Pt(II)-coordinated NH_3 and d(GpG)[27] supports that, once stacking occurs between Pt(L)(en) and NMP, the above-mentioned hydrogen bonding may be formed in solution in the present case by the cooperative effect of the stacked aromatic rings in the vicinity. Sigel[22f] pointed out that the high stability of the complex of carboxypeptidase A with its inhibitor phenylpropionate can be explained by a cooperative mechanism due to the hydrophobicity arising from the hydrophobic interaction between the phenyl moiety of the inhibitor and the hydrophobic pocket of the enzyme; as a result, the effective dielectric constant decreases and thus the polar carboxylate–Zn(II) interaction is strengthened. A reasonable explanation of the stacking interaction as a driving force for formation of Pt(L)(en)–NMP is that the stacked rings in the adduct produce a local or microscopic hydrophobicity, which makes the nearby electrostatic and hydrogen bonds more effective. We see the cooperative effects from the induced CD spectral magnitude for Pt(bpy)(en)–AMP as compared with the magnitudes for Pt(bpy)(en)–Ado and Pt(bpy)(en)–D-ribose 5-phosphate. The stability difference of 0.4 log unit between Pt(phen)(en)–AMP

(24) Naumann, C. F.; Sigel, H. *J. Am. Chem. Soc.* **1974**, *96*, 2750–2756.
(25) (a) Coloquhoun, H. M.; Stoddart, J. F.; Williams, D. J.; Wolstenholme, J. B.; Zarzycki, R. *Angew. Chem.* **1981**, *93*, 1093–1095. (b) Ballardini, R.; Gandolfi, M. T.; Balzani, V.; Kohnke, F. H.; Stoddart, J. F. *Angew. Chem.* **1988**, *100*, 712–713.
(26) (a) Mangani, S.; Orioli, P. *J. Chem. Soc., Chem. Commun.* **1985**, 780–781. (b) Poojary, M. D.; Begum, N. S.; Manohar, H.; Bau, R. *J. Chem. Soc., Chem. Commun.* **1985**, 821–822.
(27) Kozdka, J.; Petsko, G. A.; Lippard, S. J. *J. Am. Chem. Soc.* **1985**, *107*, 4079–4081.

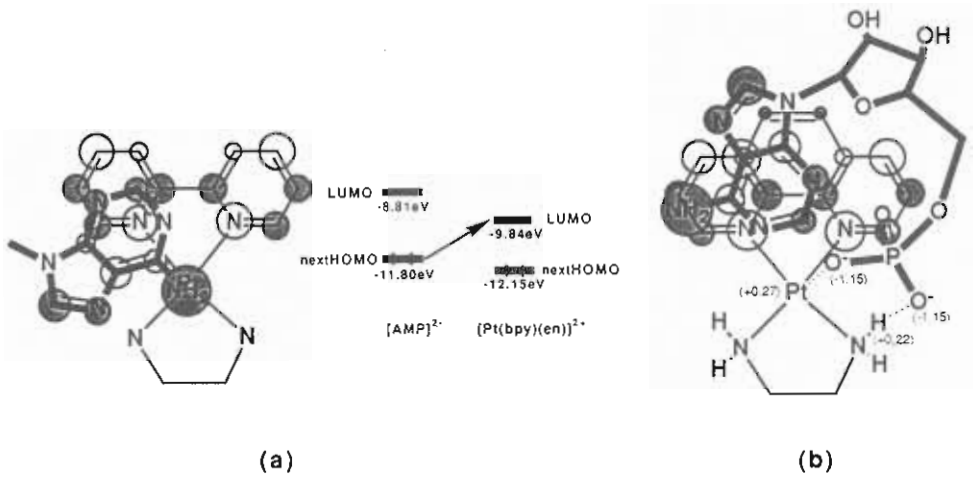

Figure 5. (a) Diagrammatic representation of the Pt(bpy)(en) (LUMO)···adenine(AMP) (nextHOMO) interaction based on the crystal structure, as given by the EHMO calculation and schematic MO diagram indicating charge transfer. (b) Proposed mode of Pt(phen)(en)···AMP adduct formation in solution with net charges shown in parentheses for Pt(II) and the amino and phosphate groups.

and –Ado (Table IV) indicates the contribution by the negatively charged phosphate group of AMP.

The pyrimidine nucleotides exhibited slightly different behavior. While the Pt(bpy)(en)–UMP system has $\Delta\delta$ values as small as 0.02–0.05 ppm, those observed for Pt(Me_4phen)(en)–CMP and –UMP are comparable with those for AMP- and GMP-containing systems, probably due to the small molecular size of the pyrimidine bases.

Comparison with the Crystal and Molecular Structure of [Pt(bpy)(en)]·AMP·10H_2O. The stacking interaction proposed in solution was established in the solid state for the crystals of Pt(bpy)(en)–AMP[20] (Figure 4). The location of the adenine ring relative to bpy corresponds well with that inferred for solution from the NMR data;[6] H-2 is close above one of the pyridine rings, whereas H-8 is outside the bpy rings. The D-ribose moiety, on the other hand, is stretched out from the Pt(II) coordination plane in the anti conformation (C2′-endo ring pucker), and the phosphate oxygen is hydrogen-bonded to the 6-amino group of a neighboring AMP molecule with the N···O distance of 2.96 Å to form alternating piles of Pt(bpy)(en) and AMP with bpy–adenine stacking at a distance of 3.5 Å. Because of the distance between the Pt(II) center and the asymmetric carbons of D-ribose, the anti conformation revealed in the solid state does not explain the observed CD activity due to the proximity effect and is not compatible with the large $\Delta\delta$ value for H-1′. The coupling constants (J) for H-1′ and H-2′, which are related to the ribose ring puckering,[5] decrease upon addition of Pt(L)(en) in the systems with AMP and GMP from 6.1 and 6.4 to 4.9 and 3.9 Hz, respectively, for L = phen, while the value is unchanged with CMP, UMP, and Ado which is devoid of the phosphate group (Table II). The results indicate that the ribose phosphate moiety in AMP and GMP undergoes a change from the C2′-endo to the C3′-endo pucker. We may therefore infer that in solution AMP assumes a syn conformation and that its ribose moiety is attracted close to the Pt(II) center. Extended Hückel molecular orbital calculation[28] indicates that formation of the Pt(bpy)(en)···adenine(AMP) adduct with the structure revealed in the solid state may be explained by the charge-transfer interaction between the π orbital of AMP^{2-} (next HOMO) and the π^* orbital of $[Pt(bpy)(en)]^{2+}$ (LUMO) (Figure 5a). On the basis of this and similar calculation we propose the mode of Pt(phen)(en)···AMP adduct formation in solution shown in Figure 5b, where we see that the phen–adenine stacking and the Pt(II)–phosphate and amino group–phosphate interactions as concluded from various lines of evidence are compatible with the nextHOMO(π)–LUMO(π^*) interaction and the net charge distribution, respectively. The structure shown in Figure 5b, which is in line with that proposed earlier,[6] is also compatible with the structure in the solid state (Figure 4) in the sense that the former can be attained by rotation of the AMP molecule with the orbital symmetry conserved and by formation of the above-mentioned polar interactions.

Concluding Remarks. The stability constants shown in Table IV indicate that the adducts are unexpectedly stable with log K values that are much larger than those reported for self-stacking of AMP (0.3)[20d] and bpy–AMP stacking (1.41).[22] This is reasonably interpreted as due to the flatness of the coordinated aromatic rings of L and the additional stabilization by the cooperativity between stacking, hydrogen bonding, and electrostatic interactions. Electron withdrawing by Pt(II) makes the electron density of L lower, which further stabilizes the adduct by favoring the CT interaction with the nucleobases. Previous calorimetric studies[7] revealed that the $\Delta H°$ vaues for Pt(L)(en)–AMP were –18.0, –25.6, and –22.9 kJ mol^{-1} for L = bpy, phen, and Me_4phen, respectively, which are greater than expected for hydrophobic interactions (–6 kJ mol^{-1}).[1a,29] This is interpreted as indicative of a stronger stacking interaction due to the CT interaction. It is interesting to note in this connection that differentiation of the hydrophobic interactions from the electrostatic ones in intercalative interactions of metal–L complexes (L = phen, bpy) into DNA have been studied by cyclic voltammetry[30] and that the hydrophobicity of L has been shown to correspond with the DNA binding ability.[31] The present observations, which are in good agreement with the results of these studies, clearly show that combination of hydrophobic and electrostatic interactions increases the adduct stability. Molecular recognitions in recently designed organic systems involving nucleic bases, nucleosides,[32] and nucleotides[33] and sequence-specific metal complex–DNA interactions[34] are excellent examples showing the effectiveness of such combination.

(28) The MO calculations were performed by using the extended Hückel molecular orbital (EHMO) method. The parameters were taken from the reported values: (a) Hoffmann, R. *J. Chem. Phys.* **1963**, *39*, 1397. (b) Hoffmann, R.; Lipscomb, W. L. *J. Chem. Phys.* **1962**, *36*, 2179. The bond lengths and angles used were those from the X-ray data determined in this work.

(29) Scheraga, H. A. *Acc. Chem. Res.* **1979**, *12*, 7–14.
(30) (a) Carter, M. T.; Bard, A. J. *J. Am. Chem. Soc.* **1987**, *109*, 7528–7530. (b) Carter, M. T.; Rodriguez, M.; Bard, A. J. *J. Am. Chem. Soc.* **1989**, *111*, 8901–8911.
(31) Pyle, A. M.; Rehmann, J. P.; Meshoyrer, R.; Kumar, C. V.; Turro, N. J.; Barton, J. K. *J. Am. Chem. Soc.* **1989**, *111*, 3051–3058.
(32) (a) Rebek, J., Jr. *Science* **1987**, *235*, 1478–1484. (b) Rebek, J., Jr. *Angew. Chem., Int. Ed. Engl.* **1990**, *29*, 245–255. (c) Tjivikua, T.; Deslongchamps, G.; Rebek, J., Jr. *J. Am. Chem. Soc.* **1990**, *112*, 8408–8414.
(33) Hosseini, M. W.; Blacker, A. J.; Lehn, J.-M. *J. Am. Chem. Soc.* **1990**, *112*, 3896–3904.
(34) (a) Youngquist, R. S.; Dervan, P. B. *J. Am. Chem. Soc.* **1985**, *107*, 5528–5529. (b) Povsic, T. J.; Dervan, P. B. *J. Am. Chem. Soc.* **1990**, *112*, 9428–9430, and references cited therein. (c) Tullius, T. D., Ed. *Metal-DNA Chemistry*; ACS Symposium Series 402; American Chemical Society: Washington, DC, 1989. (d) Sigman, D. S. *Biochemistry* **1990**, *29*, 9097–9105.

The cooperative effect of aromatic ring stacking and Pt(II)···phosphate and en···phosphate polar bonds explains the strong intercalative DNA binding by platinum intercalators[3] and Ru(phen)$_3^{2+}$.[35] The Pt(II) center has an electron-withdrawing effect on L which is similar to that of the positively charged nitrogen of typical intercalators such as ethidium bromide. Detailed calorimetric studies are being carried out in this laboratory, and they will enable us to have a deeper insight into the thermodynamic aspects of the adduct formation.

(35) (a) Barton, J. K.; Danishefsky, A. T.; Goldberg, J. M. *J. Am. Chem. Soc.* **1984**, *106*, 2172-2176. (b) Barton, J. K.; Goldberg, J. M.; Kuma, C. V.; Turro, N. J. *J. Am. Chem. Soc.* **1986**, *108*, 2081-2088. (c) Barton, J. K. *Science* **1986**, *233*, 727-734.

Acknowledgment. This work was supported by a Grant-in-Aid for Scientific Research by the Ministry of Education, Science, and Culture of Japan, to which our thanks are due.

Contribution from the Department of Chemistry, University of Washington, Seattle, Washington 98195

Oxygen Atom Transfer from a Phosphine Oxide to Tungsten(II) Compounds

Stephanie L. Brock and James M. Mayer*,[1]

Received November 13, 1990

$WCl_2(PMePh_2)_4$ (**1**) reacts rapidly with $Ph_2P(O)CH_2CH_2PPh_2$ (**5**, the monooxide of diphos) to give an adduct, $WCl_2[Ph_2P(O)CH_2CH_2PPh_2](PMePh_2)_2$ (**6**). On being heated at 80 °C for 8 h, **6** rearranges by transferring the phosphoryl oxygen to tungsten, with the formation of tungsten-oxo complexes $W(O)Cl_2(diphos)(PMePh_2)$ (**7**) and $W(O)Cl_2(PMePh_2)_3$ (**2**), as well as $WCl_2(diphos)(PMePh_2)_2$ (**8**). This is the first example of oxygen atom transfer from a phosphine oxide to a metal center, a remarkable reaction because of the strength of the P-O bond (roughly 130 kcal/mol). The presence of an oxygen atom transfer step in this reaction has been confirmed by oxygen-18-labeling studies. $WCl_2(PMe_3)_4$ (**9**) also deoxygenates **5**, forming similar tungsten-oxo complexes, but in this case an intermediate is not observed. Nonchelating phosphine oxides are unreactive with **1** and **9**, indicating that the chelating nature of **5** is needed to assist the initial coordination of the phosphoryl oxygen. The kinetic barriers to deoxygenation of phosphine oxides lie both in the initial coordination of the phosphine oxide and in the actual oxygen atom transfer step. Allyl- and vinylphosphine oxides also react with **1**, but oxygen atom transfer from these substrates has not been observed. An unusual tungsten-oxo complex with a chelating allyldiphenylphosphine oxide, $W(O)Cl_2[CH_2{=}CHCH_2P(O)Ph_2]PMePh_2$ (**13**) has been isolated and its X-ray crystal structure determined. Crystal data for **13**: a = 9.2547 (9) Å, b = 16.738 (2) Å, c = 18.023 (2) Å, β = 100.696 (9)°, monoclinic, $P2_1/c$, Z = 4.

Oxygen atom transfer reactions have received increasing attention in recent years because of their importance as fundamental steps in a variety of both stoichiometric and catalytic processes.[2-4] Examples range from the reduction of nitrate to nitrite mediated by a molybdenum enzyme[5] to the epoxidation of olefins by a number of metal-oxo complexes, including the iron-oxo center in cytochrome P-450 enzymes.[6] A variety of reagents have been used to deliver an oxygen atom to a metal center or remove oxygen from a metal.[2,3] By far, the most common reagents for oxygen atom abstraction are phosphines, PR_3, which reduce a wide range of metal-oxo complexes (eq 1).

$$L_nM{=}O + PR_3 \rightarrow L_nM + R_3P{=}O \qquad (1)$$

The reactivity of phosphines results in large part from the very strong P-O bond, 127 kcal/mol in Ph_3PO and 139 kcal/mol in Me_3PO.[7] Because of this strong bond, the oxidation of phosphines is easy to accomplish, while only strongly reducing reagents will generate phosphines from phosphine oxides (e.g., $LiAlH_4$, $PhSiH_3$).[8] The reactions reported here are the first examples of oxygen atom transfer from a phosphine oxide to a metal complex, the reverse of eq 1.[9]

Our studies of $WCl_2(PMePh_2)_4$ (**1**) have shown it to be an extremely potent oxygen atom acceptor, forming oxo complexes on reaction with water, alcohols, ketones, epoxides, SO_2, and CO_2.[10-13] The cleavage of CO_2 forms an equilibrium mixture of the oxo-carbonyl and oxo-tris(phosphine) complexes, $W(O)Cl_2(CO)(PMePh_2)_2$ and $W(O)Cl_2(PMePh_2)_3$ (eq 2),[10,11,14] a remarkable reaction because of the strength of the C-O bond that

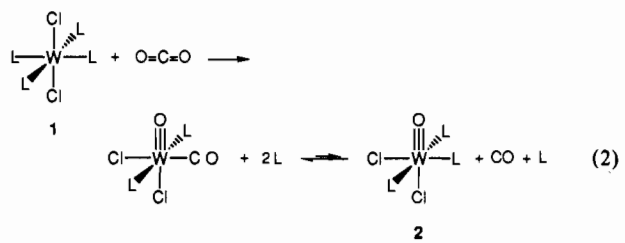

(2)

(1) Presidential Young Investigator, 1988-1993; Alfred P. Sloan Research Fellow, 1989-1991.
(2) Holm, R. H. *Chem. Rev.* **1987**, *87*, 1401-1449.
(3) Nugent, W. A.; Mayer, J. M. *Metal-Ligand Multiple Bonds*; Wiley-Interscience: New York, 1988; pp 248-251.
(4) Sheldon, R. A.; Kochi, J. K. *Metal-Catalyzed Oxidations of Organic Compounds*; Academic: New York, 1981.
(5) *Molybdenum Enzymes*; Spiro, T. G., Ed.; Wiley-Interscience: New York, 1985. Model studies: Craig, J. A.; Holm, R. H. *J. Am. Chem. Soc.* **1989**, *111*, 2111-2115. Garner, C. D.; Hyde, M. R.; Mabbs, F. E.; Routledge, V. I. *J. Chem. Soc., Dalton Trans.* **1975**, 1180-1186. Wieghardt, K.; Woeste, M.; Roy, P. S.; Chaudhuri, P. *J. Am. Chem. Soc.* **1985**, *107*, 8276-8277.
(6) *Cytochrome P-450 Structure, Mechanism, and Biochemistry*; Ortiz de Montellano, P. R., Ed.; Plenum: New York, 1986; see especially Chapter 1.
(7) Hudson, R. F. *Structure and Mechanism in Organo-Phosphorus Chemistry*; Academic: New York, 1965; pp 68-70.
(8) Hays, H. R.; Peterson, D. J. In *Organic Phosphorus Compounds*; Kosolapoff, G. M., Maier, L., Eds.; Wiley: New York, 1972; Vol. 3, pp 408-413.
(9) There are examples of *oxide* (O^{2-}) transfer from a phosphine oxide to a metal, without oxidation state changes. See, for instance: Horner, S. M.; Tyree, S. Y., Jr. *Inorg. Chem.* **1962**, *1*, 122-127.
(10) Su, F. M.; Bryan, J. C.; Jang, S.; Mayer, J. M. *Polyhedron* **1989**, *8*, 1261-1277.
(11) Bryan, J. C.; Geig, S. J.; Rheingold, A. L.; Mayer, J. M. *J. Am. Chem. Soc.* **1987**, *109*, 2826-2828.
(12) Bryan, J. C.; Mayer, J. M. *J. Am. Chem. Soc.* **1990**, *112*, 2298-2308.
(13) Jang, S.; Atagi, L. M.; Mayer, J. M. *J. Am. Chem. Soc.* **1990**, *112*, 6413-6414.
(14) The equilibrium $W(O)Cl_2(CO)(PMePh_2)_2 + PMePh_2 \rightleftharpoons W(O)Cl_2(PMePh_2)_3 + CO$ lies to the left; K_{eq} has been estimated to be 500.

0020-1669/91/1330-2138$02.50/0